Further Evidence for the Mandatory Nature of Polysaccharide Debranching for the Aggregation of Semicrystalline Starch and for Overlapping Functions of Debranching Enzymes in Arabidopsis Leaves[1][W]

Fabrice Wattebled, Véronique Planchot, Ying Dong, Nicolas Szydlowski, Bruno Pontoire, Aline Devin, Steven Ball, and Christophe D'Hulst*

Unité de Glycobiologie Structurale et Fonctionnelle, UMR8576 CNRS/Université des Sciences et Technologies de Lille, F–59655 Villeneuve d'Ascq, France (F.W., Y.D., N.S., A.D., S.B., C.D.); and UR1268 Biopolymères, Interactions, Assemblages, INRA France, F–44300 Nantes, France (V.P., B.P.)

Four isoforms of debranching enzymes are found in the genome of Arabidopsis (*Arabidopsis thaliana*): three isoamylases (ISA1, ISA2, and ISA3) and a pullulanase (PU1). Each isoform has a specific function in the starch pathway: synthesis and/or degradation. In this work we have determined the levels of functional redundancy existing between these isoforms by producing and analyzing different combinations of mutations: *isa3-1 pu1-1*, *isa1-1 isa3-1*, and *isa1-1 isa3-1 pu1-1*. While the starch content strongly increased in the *isa3-1 pu1-1* double mutant, the latter decreased by over 98% in the *isa1-1 isa3-1* genotype and almost vanished in triple mutant combination. In addition, whereas the *isa3-1 pu1-1* double mutant synthesizes starch very similar to that of the wild type, the structure of the residual starch present either in *isa1-1 isa3-1* or in *isa1-1 isa3-1 pu1-1* combination is deeply affected. In the same way, water-soluble polysaccharides that accumulate in the *isa1-1 isa3-1* and *isa1-1 isa3-1 pu1-1* genotypes display strongly modified structure compared to those found in *isa1-1*. Taken together, these results show that in addition to its established function in polysaccharide degradation, the activity of ISA3 is partially redundant to that of ISA1 for starch synthesis. Our results also reveal the dual function of pullulanase since it is partially redundant to ISA3 for degradation and to ISA1 for synthesis. Finally, x-ray diffraction analyses suggest that the crystallinity and the presence of the 9- to 10-nm repetition pattern in starch precisely depend on the level of debranching enzyme activity.

Starch accumulates in plants as huge water-insoluble, semicrystalline granules. It is composed of two macromolecules, amylose and amylopectin, which consist of Glc residues linked together by α-1,4 and α-1,6 *O*-glycosidic bonds. Amylose is an essentially linear molecule with less than 1% of α-1,6 branches. The degree of polymerization (DP) of amylose ranges between several hundreds to thousands of Glc residues. Amylopectin is a moderately branched molecule that displays 5% to 6% of α-1,6 branches. Its DP generally exceeds 10^5 Glc residues (for review, see Buléon et al., 1998). The branches of amylopectin, unlike those of glycogen, are asymmetrically distributed and are tightly spaced in specific regions defined as the amorphous lamellae. This close packing of branches supports chains that in turn are also closely packed into clusters, thus allowing them to intertwine to form helical structures and to crystallize. The type of crystalline lattice (A- or B-type) of the so-called "amylopectin clusters" can be probed by wide-angle x-ray diffraction (WAXS), whereas the respective sizes of the amorphous (the branches) and the crystalline lamellae can be investigated by small-angle x-ray scattering (SAXS). In short, the asymmetrical distribution of branches in amylopectin is responsible for the aggregation and packaging of amylopectin into semicrystalline starch granules. This defines the major differences between the structures and properties of amylopectin and glycogen, which is entirely water soluble. Amylose synthesis occurs within the starch granules and requires the presence of both granule-bound starch synthase (GBSS; Hovenkamp-Hermelink et al., 1987; Delrue et al., 1992; Nakamura et al., 1995) and a preformed semicrystalline granule (Dauvillée et al., 1999). Amylopectin synthesis on the other hand is driven by a highly complex machinery consisting of several sets of enzyme complexes, including soluble starch synthases and branching enzymes (Hennen-Bierwagen et al., 2008; Tetlow et al., 2008). The first steps of amylopectin synthesis, including elongation from ADP-Glc and branching of the elongated chains,

[1] This work was supported by Génoplante (program no. Af2001030), the Centre National de la Recherche Scientifique, the Institut National de la Recherche Agronomique, the Région Nord-Pas de Calais, the European Union-FEDER (grant ARCir and CPER to C.D.), and the Agence Nationale de la Recherche (grant no. JC5145 ACI Jeunes-Chercheurs to C.D.).

* Corresponding author; e-mail christophe.dhulst@univ-lille1.fr.

The author responsible for distribution of materials integral to the findings presented in this article in accordance with the policy described in the Instructions for Authors (www.plantphysiol.org) is: Christophe D'Hulst (christophe.dhulst@univ-lille1.fr).

[W] The online version of this article contains Web-only data.
www.plantphysiol.org/cgi/doi/10.1104/pp.108.129379

are shared by the pathways of bacterial glycogen synthesis (for review, see Morell et al., 2006). How then does one explain the differences in branching distribution between glycogen and starch? Ball et al. (1996) and Myers et al. (2000) have jointly proposed that isoamylase, a form of starch debranching enzyme (DBE), was responsible for splicing out the misplaced branches due to the action of the randomly acting branching enzymes. Because isoamylase is unable to cleave out tightly spaced branches, this would leave clusters of branches responsible for this asymmetrical distribution. This glucan trimming model was proposed to explain the phenotypes of *Chlamydomonas reinhardtii* and cereal mutants that substituted starch by glycogen synthesis. Because in *Chlamydomonas* this substitution was essentially complete, it was proposed that polysaccharide debranching was mandatory to obtain amylopectin aggregation into semicrystalline insoluble granules (Mouille et al., 1996). However, in cereals and plants the mutants displayed a milder phenotype expressivity and accumulated both glycogen and a vastly decreased yet significant amount of modified starch (James et al., 1995; Kubo et al., 2005; Wattebled et al., 2005). Very early on, it was proposed that this difference was due to the presence of other starch DBEs that impacted differently the plant and algal systems (Myers et al., 2000).

DBEs are classified in two groups depending on their substrate preferences: isoamylases and pullulanases. Pullulanases readily hydrolyze α-1,6 linkages of pullulan, a microbial polymer of maltotriosyl residues joined by α-1,6 linkages. Pullulanases that prefer such tightly spaced branches can also act on amylopectin but are poorly active on the loosely spaced branches of glycogen. Conversely, isoamylases are inactive on pullulan but do hydrolyze the α-1,6 bonds of both amylopectin and glycogen. In the Arabidopsis (*Arabidopsis thaliana*) nuclear genome, three genes encoding isoamylase-like sequences (*ISA1*, *ISA2*, and *ISA3*) and one gene encoding pullulanase (*PU1* or *LDA1*, for limit dextrinase, another name for pullulanase) were found (Delatte et al., 2005; Wattebled et al., 2005). Both *ISA1* and *ISA2* condition the presence of the same enzymatic activity that is suspected to be a heteromultimeric complex as initially suggested by the work on *Chlamydomonas* mutants (Dauvillée et al., 2001a, 2001b) and later fully demonstrated in potato tubers (*Solanum tuberosum*; Hussain et al., 2003) and rice (*Oryza sativa*; Utsumi and Nakamura, 2006). This heteromultimeric complex has also been demonstrated to be required for Arabidopsis amylopectin synthesis (Delatte et al., 2005; Wattebled et al., 2005). However, ISA1 is likely the only active subunit of the complex since ISA2 lacks mandatory amino acid residues for debranching activity (Hussain et al., 2003). The *ISA3* gene encodes an isoamylase type of DBE that is compulsory for starch degradation at night in Arabidopsis leaves. In the absence of ISA3, starch overaccumulates in leaves at the end of both day and night periods (Wattebled et al., 2005). Finally, a mutation at the *PU1* locus does not lead to obvious change regarding the starch accumulation phenotype of the corresponding plant. However, a more pronounced phenotype for the *isa2*- mutation is observed when the *pu1*- mutation is added, suggesting the existence of a low level yet significant overlap of function between both enzymes toward amylopectin synthesis (Wattebled et al., 2005) that was also reported in maize (*Zea mays*; Dinges et al., 2003).

The glucan trimming model predicts that starch synthesis should not be possible in the absence of DBEs. It also predicts that altering the activity of the normal heteromultimeric isoamylase complex should always affect deeply the structure of the residual starch that accumulates. Alternative models do not make this prediction and propose mechanisms (priming or water-soluble polysaccharide [WSP] clearing) that suggest that the residual starch should display an overall normal or only slightly and indirectly affected structure.

The objective of this work was to evaluate more precisely the level of redundancy that may exist between the different forms of DBE to explain the presence of a significant yet reduced level of starch in the higher plant isoamylase-defective mutants and to check the ability of plants to synthesize starch in the absence of measurable DBE activity. To this end combinations of mutations for DBE have been generated and characterized in Arabidopsis. The results reported here are discussed in light of DBE function in starch metabolism.

RESULTS

Generation and Selection of Double and Triple Mutant Lines

The *isa1-1 isa3-1* and *isa3-1 pu1-1* double mutants were generated by crossing the corresponding single mutant lines described in Wattebled et al. (2005). The genotypes of several tens of segregating individuals were confirmed by running reverse transcription (RT)-PCR amplifications on total RNA extracted from leaves (Supplemental Fig. S1, A and B). The triple *isa1-1 isa3-1 pu1-1* mutant combination was produced by crossing both *isa1-1 isa3-1* and *isa3-1 pu1-1* double mutants selected previously. Again, several tens of segregating individuals were selected for further characterization by RT-PCR amplifications to ensure the abolition of normal mRNA synthesis (Supplemental Fig. S1C).

To correlate mutations with the impairment of enzyme activities, specific zymograms for DBE activities were performed (Fig. 1, B and C). Iso1 (the DBE activity controlled by both *ISA1* and *ISA2* genes), ISA3, and PU1 activities were all distinctively observed in cell extract of both ecotype Wassilewskija (Ws) and ecotype Columbia (Col-0) of Arabidopsis wild-type lines (lanes 1 and 8). These enzymes were

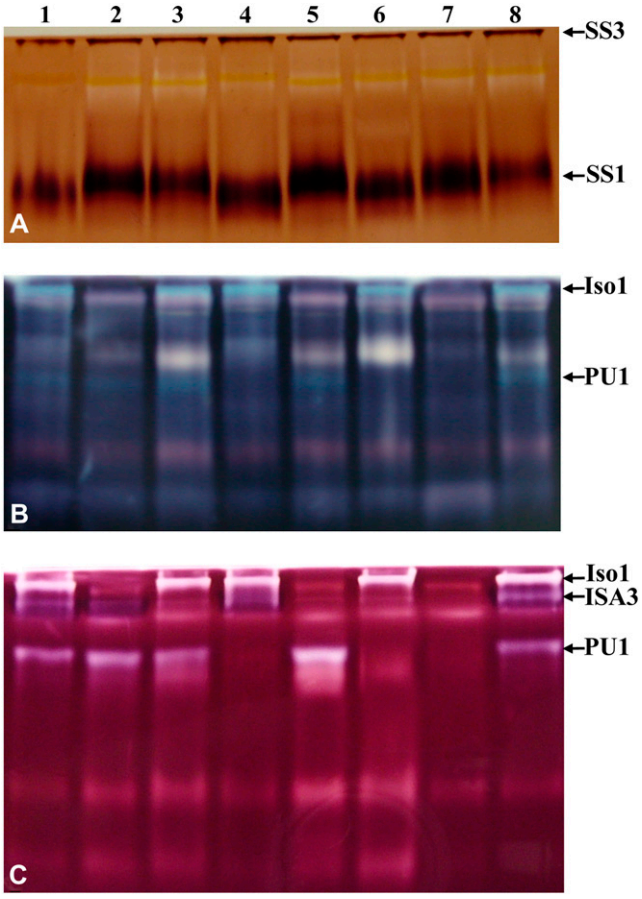

Figure 1. Zymogram analysis of mutants affected for DBE activities. A to C, Samples of soluble proteins were prepared from leaves of different wild-type and mutant plants as described in "Materials and Methods," loaded onto polyacrylamide gels impregnated with glycogen (A), potato soluble starch (B), and maize β-limit dextrins (C), and subsequently submitted to electrophoresis. After migration, the gels were incubated in the suitable buffer to allow enzymes to modify the substrate present into the polyacrylamide matrix. Enzymatic activities were then developed by soaking the gel for several minutes in lugol solution. Pictures were taken immediately after the gels were briefly rinsed in deionized water to remove iodine in excess. A, The gel was incubated in an ADP-Glc-containing buffer that is specific to soluble starch synthases. SS1 and SS3 are indicated in the picture. B and C, Gels were incubated in a Tris buffer that allows glucan-modifying enzymes to act on the substrate available within the polyacrylamide matrix. Bands corresponding to various DBEs (Iso1, ISA3, and PU1) are indicated in the picture. Lane 1, Ws; lane 2, *isa1-1*; lane 3, *isa3-1*; lane 4, *pu1-1*; lane 5, *isa1-1 isa3-1*; lane 6, *isa3-1 pu1-1*; lane 7, *isa1-1 isa3-1 pu1-1*; lane 8, Col-0.

missing from the corresponding single and combined mutant genotypes (Fig. 1, B and C, lanes 2–7).

Starch metabolizing enzymes such as ADP-Glc pyrophosphorylase (AGPase), glucan-phosphorylases, soluble starch synthases, D-enzyme, pullulanase, and amylases were tested in the different mutants either by in vitro assay or by zymogram (Table I; Fig. 1). Activities of these enzymes were not significantly changed except for pullulanase in the *isa1-1 isa3-1* double mutant and β-amylase in the *isa3-1* and *isa3-1 pu1-1* mutants, which were significantly increased when compared to those of wild-type (Ws or Col-0) and other mutants.

At the level of growth and development, no effect was recorded on seed germination, growth rate, plant size, organ morphologies, flowering, and silique formation when plants were cultured under 16-h-day/8-h-night or 12-h-day/12-h-night regimes in greenhouse or climatic chambers, respectively.

Characterization of α-Glucan Accumulation

Starch (referred to here as Percoll-purified insoluble glucans) and WSP (soluble glucans from perchloric acid extraction) levels were quantified at the end of the light period for plants cultivated in a 16-h photoperiod (Table II). As already reported by Wattebled et al. (2005), starch content was unchanged in *pu1-1*, strongly reduced in *isa1-1*, and increased in *isa3-1* (Table II). The WSP content was not significantly different in both *isa3-1* and *pu1-1* compared to the wild type but was strongly increased in *isa1-1* (Table II). Starch content in line *isa1-1 isa3-1* was very low, being only 1.7% of that of the wild type. This corresponds to an 80% to 90% decrease in starch relative to the single *isa1-1* mutant. WSP contents were roughly the same in both *isa1-1* and *isa1-1 isa3-1* mutants. The presence of a tiny but significant amount of Percoll-purified water-insoluble glucans was detected in line *isa1-1 isa3-1 pu1-1* at the end of the day. This level represents less than 1/40th of that found in the double *isa1-1 isa3-1* mutant. Indeed, the level of water-insoluble glucans in the triple mutant was 0.0031 ± 0.0001 mg g^{-1} of fresh weight (FW; $n = 3$), which is about 0.04% of the wild-type level. The measure was highly reproducible over three independent experiments carried out during this work. Therefore, it can be considered as specific to this genotype. Conversely, the WSP content was increased in that triple mutant, being 2.5 times higher than that of both *isa1-1* and *isa1-1 isa3-1* mutants at the end of the day.

The starch content was higher in the *isa3-1 pu1-1* double mutant when compared to that of *isa3-1*. This result argues for a function of pullulanase in degradation that is not observed when an active form of the ISA3 protein is still present (no obvious impact on starch content was observed in *pu1-1*; Wattebled et al., 2005).

Changes in starch content in a 12-h photoperiod (for plants cultivated in climatic chambers) were recorded for *isa3-1 pu1-1* and *isa1-1 isa3-1* and compared to those of other DBE mutants and wild-type references (Fig. 2). Whatever the time point of the cycle, the starch level remains always higher in this double mutant compared to *isa3-1* and therefore to the wild type (Fig. 2A). The rate of degradation at night appears slightly lower than the rate of synthesis during the day in both *isa3-1* and *isa3-1 pu1-1* mutants. This situation is dif-

Table I. *In vitro assay of starch metabolizing enzymes performed with leaf extracts of wild-type and mutant plants*

Activities are expressed in nmol min^{-1} mg^{-1} of proteins (mean value ± SE; $n = 3$).

	Ws	Col-0	*isa1-1*	*isa3-1*	*pu1-1*	*isa1-1 isa3-1*	*isa3-1 pu1-1*	*isa1-1 isa3-1 pu1-1*
AGPase[a]	74.2 ± 12.9	93.1 ± 24.6	91.7 ± 17.6	99.6 ± 25.0	61.2 ± 12.2	100 ± 27.5	79.7 ± 12.5	78.0 ± 18.9
Phosphorylase	9.6 ± 2.4	8.0 ± 2.0	7.6 ± 1.6	8.5 ± 0.6	7.3 ± 0.9	10.9 ± 1.3	12.5 ± 0.7	10.2 ± 0.5
D-Enzyme	40.5 ± 2.2	38.7 ± 1.3	46.3 ± 2.1	45.4 ± 2.6	35.9 ± 1.0	37.6 ± 0.6	41.0 ± 0.9	47.5 ± 0.7
α-Amylase	33.7 ± 4.1	32.3 ± 3.9	28.7 ± 3.9	39.3 ± 4.2	33.1 ± 2.4	47.2 ± 3.4	31.9 ± 0.5	30.9 ± 2.8
β-Amylase	140 ± 5	176 ± 12	217 ± 11	357 ± 42	140 ± 30	119 ± 33	176 ± 28	427 ± 114

[a]Measured in the presence of 1.5 mM 3-phosphoglyceric acid.

ferent to that observed for the wild-type, *pu1-1*, and *isa1-1* lines, for which both synthesis and degradation occur at the same rate (absolute values) and for which the starch level is back to zero at the end of night (Fig. 2, A and B). For the *isa1-1 isa3-1* double mutant, the starch content was always very low compared to that of the wild type whatever the time point of the cycle, except at the end of the night where the starch content in both lines was back to undetectable levels (Fig. 2B). Because of the very tiny level of Percoll-purified insoluble α-glucans found in *isa1-1 isa3-1 pu1-1* even after 16 h of illumination, it was not possible to provide accurate and consistent data for this line over a 12-h-day/12-h-night cycle.

As expected, WSP accumulation was maximal in *isa1-1*, *isa2-1*, and *isa2-1 pu1-1* at the end of the day (Fig. 3A). However, the WSP content was very low at the end of the night in these lines and comparable to those of the wild type or the *isa3-1* and *pu1-1* single mutant lines. Despite the low level of material measured, it should be emphasized that the time course of the WSP content in *isa3-1 pu1-1* was different from that witnessed in other lines. Indeed, WSP levels were maximal at the end of the dark, but minimal at the end of the day and the beginning of the dark period (as shown in Fig. 3B). This argues for distinctive modes of WSP production in *isa3-1 pu1-1* when compared to *isa1-1* for instance. This behavior could be related to the important drop in starch breakdown that occurs in the *isa3-1 pu1-1* double mutant since two of the major DBE forms involved in starch breakdown were lacking.

In the triple mutant, WSP content was increased when compared to the wild type, whatever the time of the cycle (Fig. 3, A and C). However, in 12-h photoperiod growth conditions, WSP content at the end of the day was lower than that measured when plants were cultivated in a 16-h-light/8-h-dark regime. Note that the time course of WSP content in the triple mutant combination resembles that of *isa3-1 pu1-1* but at a much higher level. Again, this argues for different modes of WSP production, relative to those present in *isa1-1* and *isa2-1* single mutants or the *isa2-1 pu1-1* double mutant line. Moreover, even after an extended exposition to darkness (108 h), the presence of a high amount of WSP was still assessed in this line (above 1 mg g^{-1} of FW; Fig. 3C). In comparison, the amount of WSP in *isa1-1*, *isa2-1*, *isa2- pu1-1*, and *isa1-1 isa3-1* mutants was back to a very low level (i.e. almost zero) only after 12 h in the dark.

To check if other sources of carbon and energy were available in *isa1-1 isa3-1 pu1-1*, variation of Glc, Fru, and Suc contents was also investigated in this line (Fig. 4). Suc and Glc contents were maximal at the end of the day before a rapid decrease at night to reach a minimum after 12 h in the dark. The Glc content was relatively constant throughout the whole dark period being always close to 0.05 mg g^{-1} of FW even after 108 h in the dark. Suc was still observed in leaves at a low level (0.02 mg g^{-1} of FW) even after 108 h of darkness exposure. After being maximal at midday, Fru content regularly decreased during the second part of the day and during the night to reach undetectable levels after

Table II. *Starch and WSP contents in the wild type (Col-0) and mutant plants (measured at the end of a 16-h light period)*

Starch refers here to Percoll-purified insoluble glucans. Values are expressed as the means of n independent measurements (independent samples) ± SE. ND, Not determined.

	Col-0	*isa1-1*	*isa3-1*	*pu1-1*	*isa1-1 isa3-1*	*isa3-1 pu1-1*	*isa1-1 isa3-1 pu1-1*
Starch quantity (mg/g leaves)	100% ($n = 4$)	11% ± 3.5 ($n = 4$)	134% ± 26 ($n = 4$)	118% ± 17 ($n = 3$)	1.7% ± 0.3 ($n = 4$)	200% ± 35 ($n = 3$)	0.038% ± 0.005 ($n = 3$)
λ_{max} of the iodine-starch complex (nm)	554 ± 1 ($n = 3$)	ND	ND	ND	ND	ND	577 ± 5 ($n = 3$)
Percentage of amylose	23% ± 7 ($n = 4$)	33% ± 5 ($n = 4$)	26% ± 6 ($n = 3$)	24% ± 7 ($n = 3$)	35% ± 6 ($n = 4$)	24% ± 4 ($n = 3$)	44% ± 5 ($n = 3$)
WSP (mg/g leaves)	0.04 ± 0.02 ($n = 4$)	2.1 ± 1.3 ($n = 4$)	0.05 ± 0.04 ($n = 4$)	0.07 ± 0.01 ($n = 3$)	2.4 ± 1.5 ($n = 4$)	0.27 ± 0.15 ($n = 3$)	6.98 ± 0.28 ($n = 3$)

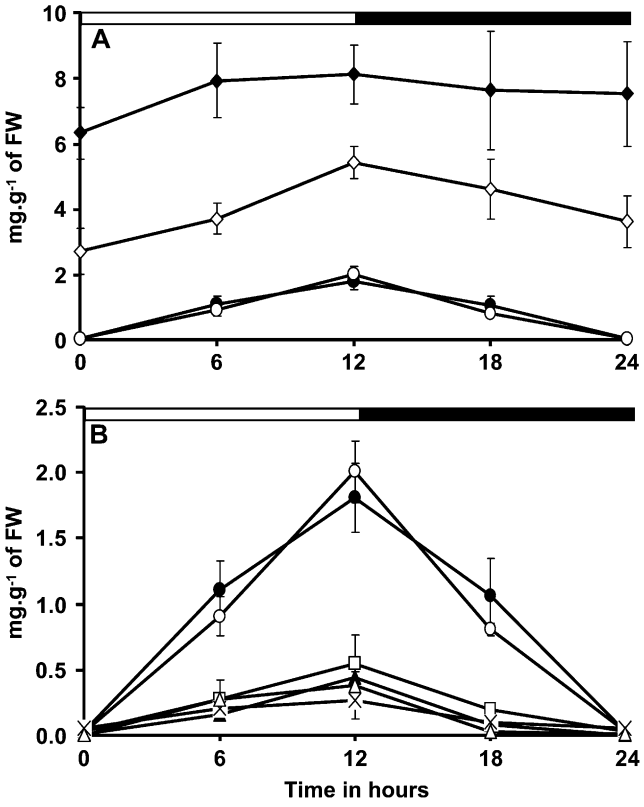

Figure 2. Time course of leaf starch content through a 12-h-day/12-h-night cycle. Arabidopsis plants were cultivated in growth cabinet as described in "Materials and Methods." Starch content was measured on leaves of three independent batches of 4-week-old plants cultivated in the same conditions. A and B, Black and white bars at the top indicate light and dark periods, respectively. Starch content is expressed in mg g^{-1} FW (leaf FW; *y* axis). Values are the means of three independent extractions. Vertical bars represent SE. For *isa2-1* and *isa2-1 pu1-1* mutants, SE is smaller in size than the symbols used. Symbols used are: ●, wild type; □, *isa1-1*; ▲, *isa2-1*; ◊, *isa3-1*; ○, *pu1-1*; △, *isa2-1 pu1-1*; ×, *isa1-1 isa3-1*; ♦, *isa3-1 pu1-1*.

12 h in the dark. No Fru was measured in leaves during the extended period of dark.

Insoluble α-Glucan Structure Determination

Starch and water-insoluble materials that accumulate in the different mutants were extracted from leaves, separated from other cell components by isopicnic centrifugation on Percoll, and solubilized in NaOH 10 mM. The λ_{max} of the starch-iodine complex was measured for both the wild-type and *isa1-1 isa3-1 pu1-1* samples (Table II). Wild-type starch displays a λ_{max} value with iodine of 554 nm (classically observed for this type of sample), whereas the λ_{max} of the triple mutant starch shows iodine of 577 nm. This increase is generally characteristic of a general increase in the average length of the starch-forming glucans. It can thus correspond to an increase in the amylose contents or to an increase in the average size of the glucans of amylopectin. Starch samples were fractionated by size exclusion chromatography on a Sepharose CL-2B column. The profiles of wild-type (1 mg), *isa1-1 isa3-1* (1 mg), and *isa1- isa3- pu1-* (0.45 mg) starches are shown in Figure 5. All profiles were similar and composed of both high (first eluted peak corresponding to amylopectin) and low (second eluted peak corresponding to amylose) M_r glucans. Surprisingly the λ_{max} values of the amylopectin-iodine complexes measured for both *isa1-1 isa3-1* and *isa1-1 isa3-1 pu1-1* were very close to that of the wild type (i.e. about 550 nm). This is different from the values reported for *isa1-* and *isa2-* mutant amylopectin as described by Wattebled et al.

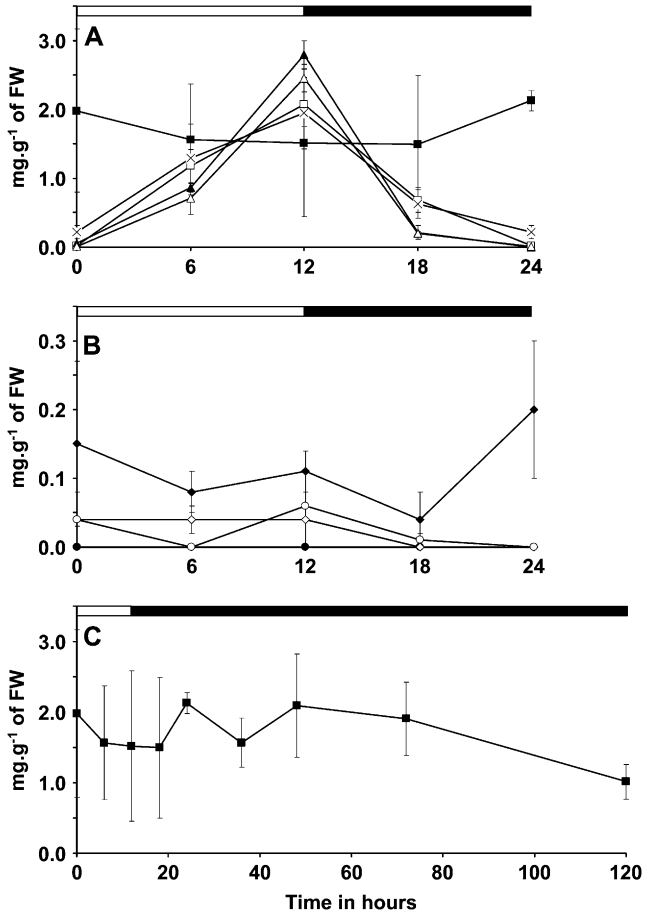

Figure 3. Time course of WSP contents in DBE mutants grown in 12-h-day/12-h-night cycles. Plants were grown in growth cabinet as described in "Materials and Methods." Black and white bars at the top of the panels indicate illuminated and dark periods, respectively. Vertical bars represent SE calculated for each time point. WSP contents were determined after extraction with perchloric acid on three independent batches of plants cultivated under the same conditions. Leaves were harvested on 4-week-old plants. C, The WSP content in the *isa1-1 isa3-1 pu1-1* mutant was determined after plants were left for an additional 108 h in the dark. Note that the *y* scale in B is 10 times smaller than that in A and C. Symbols used are: ●, wild type; □, *isa1-1*; ▲, *isa2-1*; ◊, *isa3-1*; ○, *pu1-1*; △, *isa2-1 pu1-1*; ×, *isa1-1 isa3-1*; ♦, *isa3-1 pu1-1*; ■, *isa1-1 isa3-1 pu1-1*.

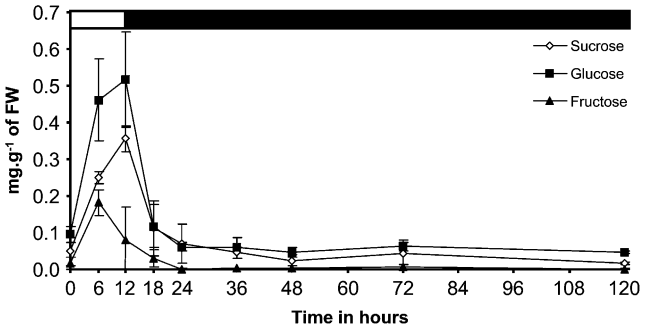

Figure 4. Variation of sugars content in the *isa1-1 isa3-1 pu1-1* mutant cultivated in 12-h-day/12-h-night cycles. Plants were grown in growth cabinet as described in "Materials and Methods." Black and white bars at the top of the panels indicate illuminated and dark periods, respectively. Vertical bars represent SE calculated for each time point. Sugars contents were determined after extraction with perchloric acid on three independent batches of plants cultivated under the same conditions. Leaves were harvested on 4-week-old plants. White diamonds, Suc; black squares, Glc; black triangles, Fru.

(2005), which were significantly higher than that of the wild type.

Fractions corresponding to amylopectin and amylose were pooled separately and both polymers were assayed. The amylose contents were increased in the mutants displaying low and very low starch content and reached up to 45% in the *isa1-1 isa3-1 pu1-1* triple mutant combination (Table II). However, the amylose content was normal in *isa3-1*, *pu1-1*, and *isa3-1 pu1-1* double mutant in which the starch content was not affected or increased compared to that of the wild type (Table II).

The structure of the purified amylopectin was further investigated after its complete enzymatic debranching. The linear glucans, produced after such a treatment, were analyzed by high-performance anion-exchange chromatography-pulsed amperometric detection (HPAEC-PAD; Dionex) to establish the chain-length distribution (CLD) profile for each sample as displayed in Figure 6. As reported by Wattebled et al. (2005), the structure of amylopectin does not appear significantly modified in *pu1-1* (Fig. 6B) compared to the wild type (Fig. 6A). Indeed, the slight differences observed in comparison to the wild-type profile generally range below 0.5 point, a level that is more or less similar to that of SE calculated for each DP for the wild type. A slightly increased number of DP3-4 glucans was monitored in the *isa3-1* mutant (Fig. 6D). An extensive increase in the range of DP3-9 glucans was also monitored in the *isa3-1 pu1-1* double mutant (Fig. 6F). This increase probably reflects the lower capacity of both mutants in removing very short glucans during starch degradation.

The amylopectin CLD of the *isa1-1* mutant was modified as already reported in Wattebled et al. (2005) with an increase in the number of DP6-9 chains (Fig. 6C). More interestingly, the modification of the amylopectin CLD in the *isa1-1 isa3-1* double mutant (Fig. 6E) was even stronger when compared to that of the *isa1-1* mutant. Indeed, this double mutant displays more or less the same increase in DP6-9 chains as in *isa1-1* along with a much stronger increase in the number of DP3-5 glucans with a maximum at DP3 (of about 3.5 points compared to the wild type and 3 points compared to *isa1-1*). The relative frequency of other glucans is less profoundly yet significantly modified, showing a relative decrease in the number of DP11-17 and DP23-31 glucans.

The CLD profile of amylopectin of the *isa1-1 isa3-1 pu1-1* mutant was obtained and compared to that of the wild type (Fig. 6G). Dramatic modifications when compared to the wild type or any other DBE mutants analyzed in this work were recorded. DP3-8 glucans were overrepresented, whereas DP11-17 and DP21-35 glucans were less frequent. Indeed, DP3 glucans were 10 times more frequent in the mutant amylopectin than in the wild type. Despite this modification, it must be emphasized that the discontinuity in glucan frequency that exists between DP17 and DP18, which is a universal feature among all amylopectins studied to date in Arabidopsis (with the noticeable exception of the *ss1-* mutants described by Delvallé et al. [2005]), was also observed in the triple mutant. This profile is original and, to our knowledge, has not been observed elsewhere. This observation makes a potential contamination of the culture by a nonmutant plant very unlikely (approximately 2,500 plants were necessary to extract sufficient amount of insoluble material to carry out its structural analysis).

Finally, amylopectin fractions from both *isa1-1 isa3-1* and *isa3-1 pu1-1* mutants were subjected to β-amylolysis before debranching (we did not have enough of the Percoll-purified insoluble material of the *isa1-1 isa3-1 pu1-1* mutant to perform this type of experi-

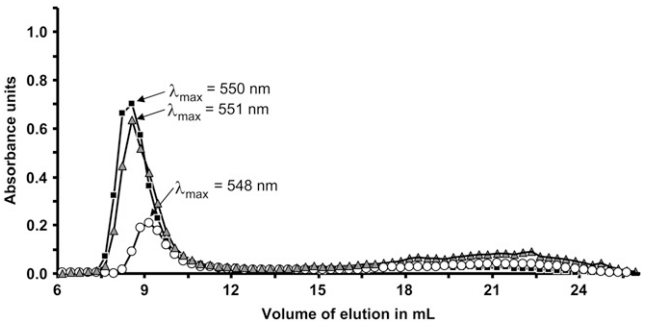

Figure 5. Size exclusion chromatography on Sepharose CL-2B matrix of Percoll-purified insoluble polysaccharides extracted from leaves at the end of the light period. Black squares, Col-0 (1 mg); white circles, *isa1- isa3- pu1-* (0.45 mg); gray triangles, *isa1-1 isa3-1* (1 mg). Starches were dissolved in NaOH 10 mM and fractions were collected at a flow rate of 12 mL h^{-1}. Each fraction was then analyzed for glucan content by complexation with iodine solution (0.2% I_2/2% KI). *x* axis, volume of elution in mL; *y* axis, maximal absorbance of the iodine-polysaccharide complex.

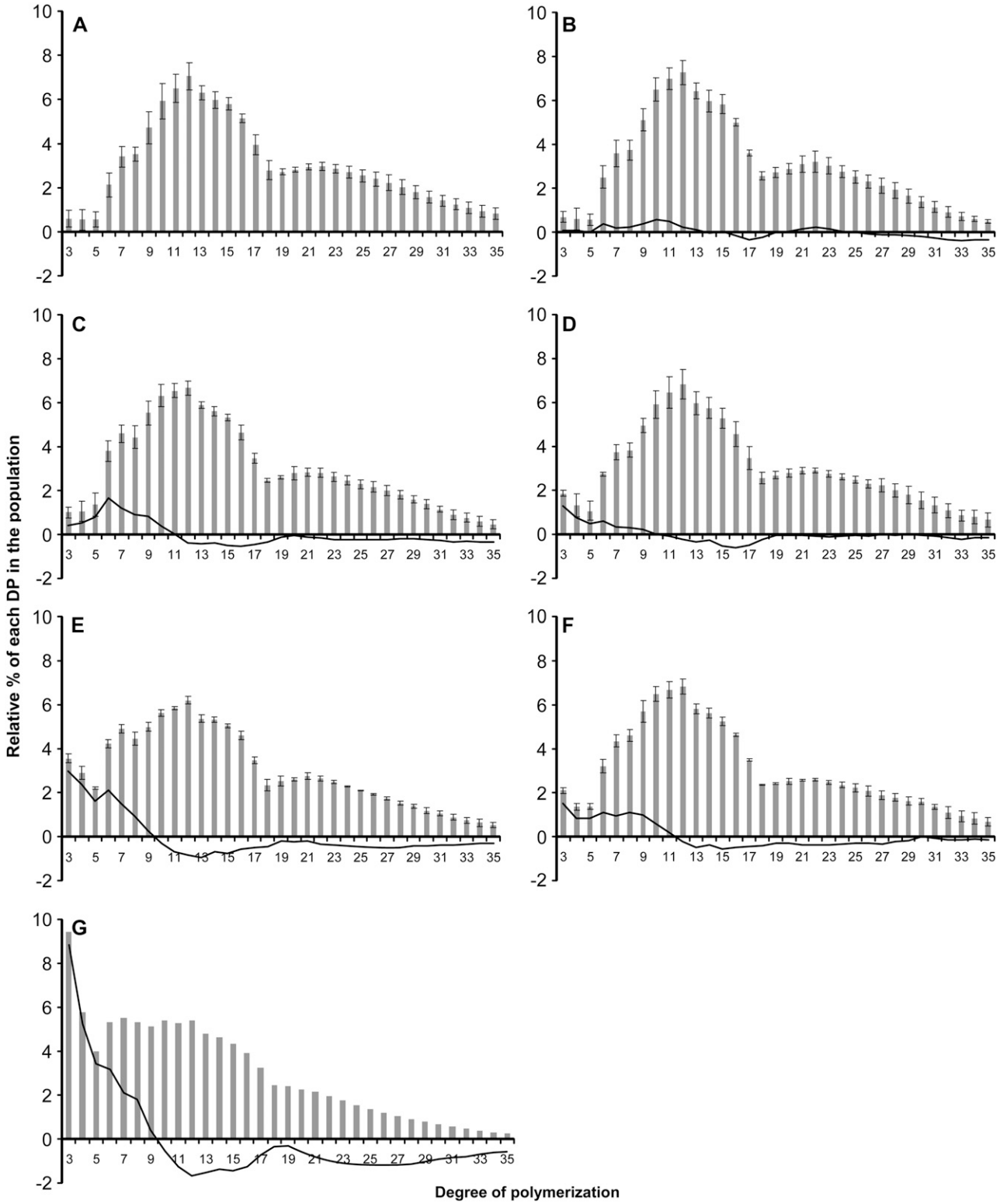

Figure 6. CLD analysis of debranched amylopectin from the wild type and DBE mutants. CLD of debranched amylopectin was obtained by HPAEC-PAD. *x* axis, DP; *y* axis, relative percentage of each DP in the whole population analyzed (vertical gray bars). Black vertical bars indicate SE. The continuous black lane is the difference plot between the mutant and the wild-type profiles (i.e. mutant profile minus wild-type profile). A, Wild type ($n = 10$); B, *pu1-1* ($n = 5$); C, *isa1-1* ($n = 3$); D, *isa3-1* ($n = 3$); E, *isa1-1 isa3-1* ($n = 3$); F, *isa3-1 pu1-1* ($n = 3$); G, *isa1-1 isa3-1 pu1-1* ($n = 2$); *n* is the number of independent repetitions.

ment). β-Amylases are exoamylases that degrade α-glucans starting from their nonreducing ends by the recurrent hydrolytic cleavage of one α-1,4 glycosidic bond out of two, thus releasing maltose. However, β-amylase activity is blocked by branches (α-1,6 linkages). The enzyme stops hydrolysis two to four Glc residues ahead of an external branch point on the chains generated by these branches or on those that support the aforementioned external branches, thereby producing a branched polymer resistant to further digestion by β-amylase, which is called a β-limit dextrin. Therefore, after debranching and analysis of the debranched products by HPAEC-PAD, a CLD profile of the core structure of amylopectin is obtained. This profile can be compared to that obtained for the same line before β-amylolysis or to that of the wild type after β-amylolysis as shown in Figure 7. In Figure 7A, the profiles correspond to the subtraction of the profile after β-amylolysis by the profile before β-amylolysis for the wild type, *isa1-1 isa3-1*, and *isa3-1 pu1-1*. Wild-type and *isa3-1 pu1-1* profiles resemble each other, showing more or less the same increase in the number of DP4-8 and DP17-20 glucans and the same decrease in the number of DP10-16 and DP22-34 glucans after β-amylolysis. The profile is different for the *isa1-1 isa3-1* mutant. In that latter case, although DP4-8 chains are increased and DP12-16 and DP22-34 chains are decreased as in the wild type, DP17-20 chains are not increased after β-amylolysis. Moreover, the profiles of *isa3-1 pu1-1* and *isa1-1 isa3-1* after β-amylolysis compared to that of the wild type were clearly distinct (Fig. 7B). Although the *isa3-1 pu1-1* mutant displays no significant difference with the wild type (differences are below the SE typically calculated for each DP), the profile of the *isa1-1 isa3-1* mutant is obviously different as witnessed by the difference plot shown in Figure 7B. This result suggests that the core structure of amylopectin in the *isa3-1 pu1-1* mutant is comparable to that of the wild type. This is obviously not the case for *isa1-1 isa3-1*, for which a modification is observed in comparison to the wild type.

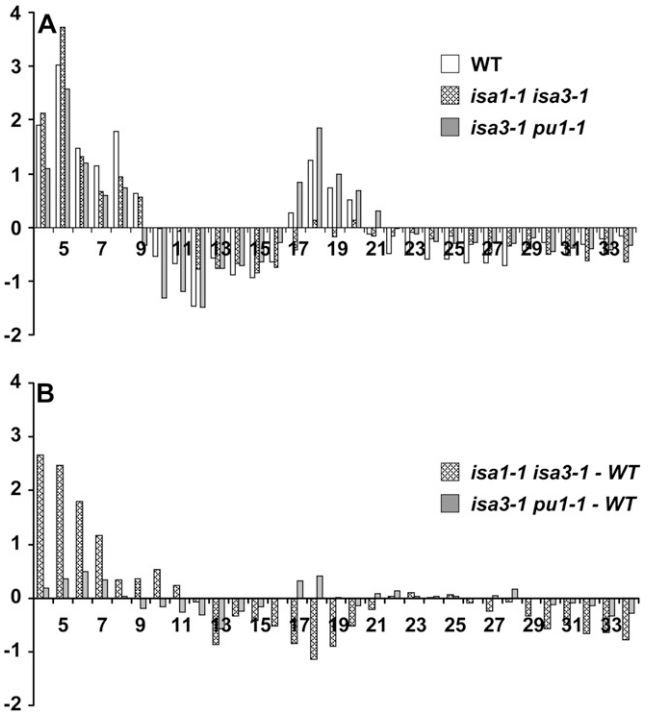

Figure 7. β-Amylolysis experiments carried out on purified amylopectin from *isa1-1 isa3-1* and *isa3-1 pu1-1* double mutants. After purification, amylopectin was submitted to degradation by β-amylase and subsequent enzymatic debranching. Linear chains were then subjected to HPAEC-PAD. A, Differential plots before and after β-amylolysis (i.e. profile after β-amylolysis minus profile before β-amylolysis) for amylopectin of wild-type, *isa1-1 isa3-1*, and *isa3-1 pu1-1* lines. B, Differential plots between mutant and wild-type amylopectin after β-amylolysis (i.e. profile of mutant amylopectin after β-amylolysis minus profile of wild-type amylopectin after β-amylolysis).

Soluble α-Glucan Structure Determination

WSPs that accumulate in the *isa1-1*, *isa1-1 isa3-1* and *isa1-1 isa3-1 pu1-1* mutants were extracted by the perchloric acid method from leaves harvested at the end of the light period from plants grown in a 16-h photoperiod. First, WSPs were purified by size exclusion chromatography on a Sephadex TSK HW50 column. The presence of glucans in the fractions was assessed by the phenol-sulfuric acid method (Supplemental Fig. S2). Second, glucans that eluted at the same volume as rabbit liver glycogen were analyzed for CLDs by HPAEC-PAD after debranching and compared to that of glycogen. The profiles of both rabbit liver glycogen and WSP of *isa1-1* are shown in Figure 8, A and B, respectively. As already reported, DP7 was in both cases the most abundant glucan in the population under analysis (Wattebled et al., 2005). A spectacular increase was observed in the abundance of DP3-4 glucans in both *isa1-1 isa3-1* and *isa1-1 isa3-1 pu1-1* mutants when compared to *isa1-1* and glycogen (Fig. 8, C and D, respectively). Conversely, DP7-16 glucans were less abundant in both mutants compared to *isa1-1*. Moreover, we have analyzed the structure of WSP in *isa1-1 isa3-1 pu1-1* at the end of night (Fig. 8E). The general structure is comparable to that of WSP purified at the end of the day (Fig. 8D). However, the number of DP3 was still increased, while the number of longer glucans was maintained or decreased. In all cases, profiles of WSP that accumulate in the *isa1-1 isa3-1* and *isa1-1 isa3-1 pu1-1* mutants bear a resemblance to the profile classically obtained with wild-type amylopectin submitted to degradation by β-amylases before debranching.

Impact of the Mutations on Starch Granule Morphology and Crystallinity

When sufficient quantities were available, the morphology of the various types of starches was analyzed by scanning electron microscopy (SEM) and transmis-

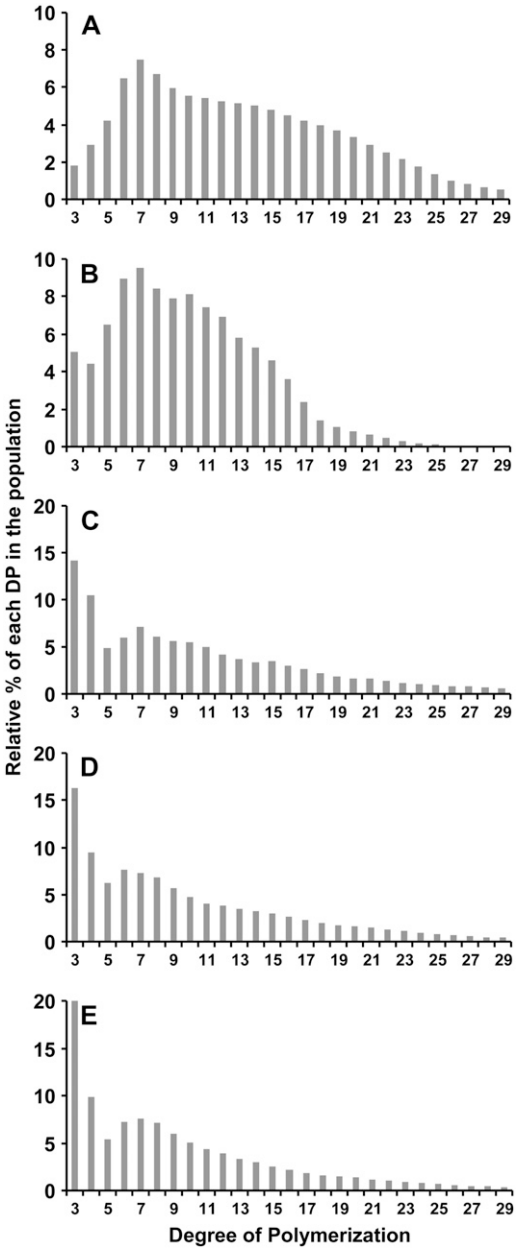

Figure 8. Comparison of CLD profiles of debranched rabbit glycogen and debranched WSP from DBE mutants. Profiles were obtained after enzymatic debranching of rabbit liver glycogen and WSP submitted to HPAED-PAD analysis. WSP were extracted by the perchloric acid method from leaves at the end of the day (except for E extracted at the end of night) from plants cultivated under 16-h-day/8-h-dark conditions (4-week-old plants). *x* axis, DP; *y* axis, relative percentage of each DP in the whole population analyzed. A, Rabbit liver glycogen ($n = 2$); B, *isa1-1* ($n = 2$); C, *isa1-1 isa3-1* ($n = 2$); D and E, *isa1-1 isa3-1 pu1-1* ($n = 2$); *n* is the number of independent repetitions. Note that the *y* scale in C, D, and E is twice bigger than that in A and B.

sion electron microscopy (TEM) on ultrathin slices. It was not possible to observe starch in the *isa1-1 isa3-1 pu1-1* triple mutant because it was impossible to obtain a sample sufficiently clean and free of various residues of extraction even after purification by isopicnic centrifugation on Percoll gradient.

Therefore, the morphology of starches from the wild-type, *isa1-1*, *isa3-1*, *pu1-1*, *isa1-1 isa3-1*, and *isa3-1 pu1-1* lines was investigated by SEM and TEM. As seen in Figure 9, wild-type granules display a smooth rather flat-shaped form that is characteristic of Arabidopsis transitory starch. The same structure was observed for both *isa3-1* and *pu1-1* mutants. However, irregularly shaped starch granules were observed in the *isa3-1 pu1-1* double mutant as seen on SEM pictures. Although the granule size was not obviously changed in these double mutant plants, their morphology appeared puffed up compared to that of wild type, *isa3-1*, and *pu1-1*.

On the contrary, dramatically smaller starch granules were observed in both *isa1-1* and *isa1-1 isa3-1* mutants. Granules were generally smaller than 1 μm in diameter with only few examples of larger starch granules. These granules display a round irregular shaped form instead of the smooth and flat morphology of the wild-type granules.

Crystallinity parameters of starch were uncovered by both SAXS and WAXS analysis (results are summarized in Fig. 10; Table III). All starch materials analyzed in this work present a B-type crystallinity. This is a common feature of starches from Arabidopsis leaves (all starches that we have analyzed to date are of B-type). Mutation at the *PU1* locus has no obvious impact on the crystallinity of starch that accumulates in the mutant. The level of crystallinity was weakly but significantly reduced in *isa2-1* (35%) and more pronouncedly in both *isa3-1* and *isa3-1 pu1-1* mutants (30% and 31%, respectively) in comparison to the wild type. Nevertheless, in all cases the signal corresponding to the 9- to 10-nm repetition of starch was still present (the 9- to 10-nm repetition corresponds to the recurrent succession of amylopectin clusters in which size is of about 9–10 nm as described by Jenkins et al. [1993]). Finally, the residual starch of the double mutant *isa1-1 isa3-1* exhibits a much lower level of crystallinity (23%) compared to the wild type, but here again, the signal of the repetition at 9 to 10 nm was still present although less pronounced than in other lines.

DISCUSSION

In this work, we have analyzed the starch accumulation phenotypes of several mutant lines of Arabidopsis lacking two or three isoforms of starch DBEs and have compared them to the wild type and corresponding single mutants. Albeit the understanding of the function of these enzymes has progressed in the last decade, different higher plant and green algal systems display distinctive expressivities of mutant phenotypes leading to contradictory interpretations. One possible explanation for these small yet significant differences can be found if different DBE isoforms display some level of functional overlap. In that case if

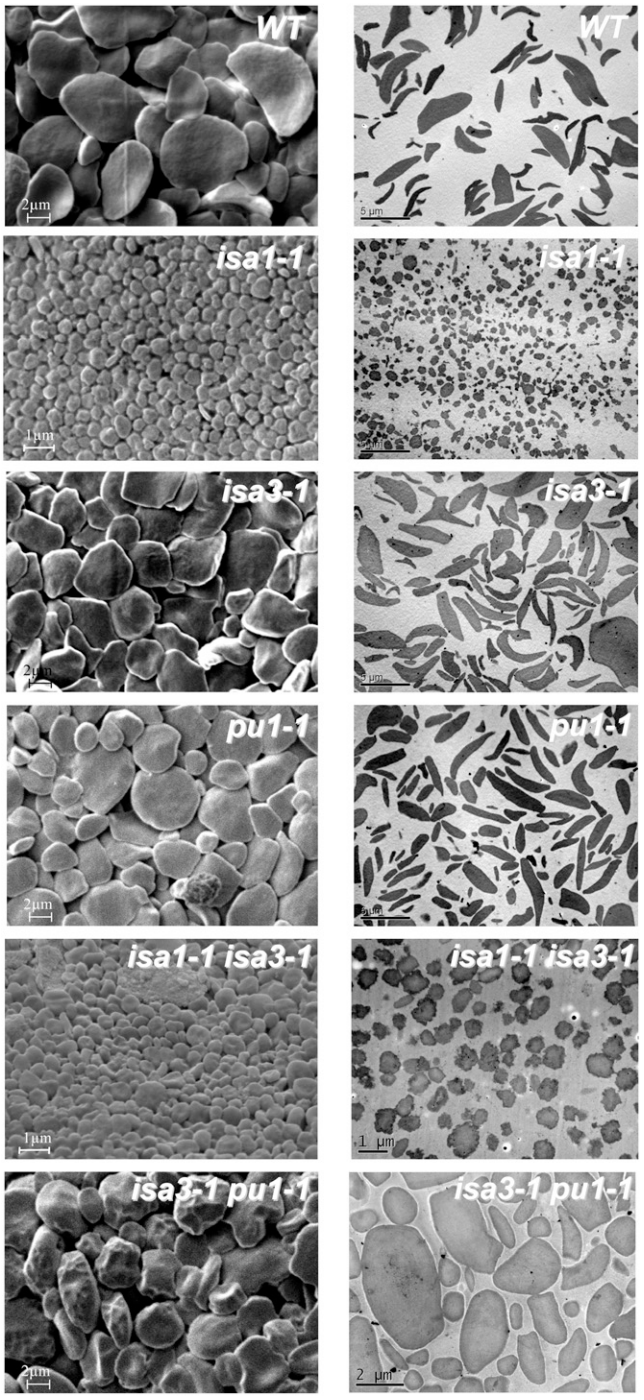

Figure 9. Electronic microscopy of purified starch granules. SEM pictures in the left column and TEM pictures in the right column on Percoll-purified starch granules prepared as described in "Materials and Methods." Scale bars (1, 2, or 5 μm) are shown in each picture.

the balance between these isoforms or their degree of functional redundancy varies from one species to another then these small differences might be explained and the contradictions may be resolved. To this end, *isa3-1 pu1-1*, *isa1-1 isa3-1*, and *isa1-1 isa3-1 pu1-1* mutants were produced by crosses and subsequently analyzed for starch accumulation.

Before going further into this discussion, it seems important to specify at this stage that, as we always do both for Chlamydomonas or Arabidopsis, we undertook the analysis of insoluble α-glucans only after we purified them by isopicnic centrifugation on Percoll gradients. Indeed, it appeared very important to complete characterizations on macromolecular objects which features were as close as possible to those that define starch (such as that purified from the wild type or previously characterized mutant lines). This approach was actually of prime importance in that case because some DBE mutants accumulate large quantities of WSPs in their chloroplasts. Under the constraint of high concentrations, some of these WSPs could precipitate in situ to form insoluble aggregates (such as those that can be observed by TEM on Arabidopsis leaf thin slices; Delatte et al., 2005). Therefore, to distinguish starch-like structures from these insoluble aggregates of WSPs, it was imperative to carry out such purification by isopicnic centrifugation (starch and WSPs do not share the same density). Thus, this approach allowed us to isolate insoluble polysaccharides whose macromolecular features were essentially preserved free of contamination by aggregated polysaccharides of the otherwise WSP fractions.

ISA3 and PU1 Have Redundant Function for Starch Degradation

The production and analysis of the *isa3-1 pu1-1* double mutant shows undoubtedly that ISA3 and PU1 have functions at least partially redundant for the degradation of transitory starch in Arabidopsis leaves. Indeed, the main effect of the combination of *isa3-1* and *pu1-1* mutations consists of a spectacular increase

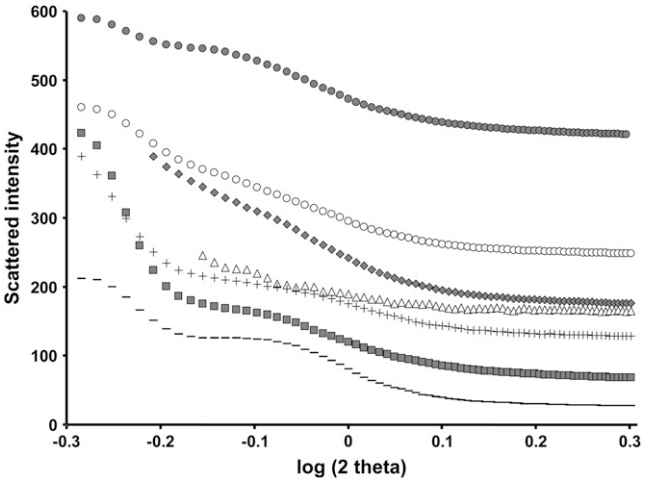

Figure 10. SAXS analysis of starches purified from different DBE mutants. Intensity of diffraction (*y* axis) is plotted against the log of 2 θ-angle (*x* axis). Symbols used are: –, wild type; △, *isa1-1*; gray symbols, *isa2-1*; ■, *isa3-1*; +, *pu1-1*; ○, *isa1-1 isa3-1*; ●, *isa3-1 pu1-1*.

Table III. *Crystallographic analysis of starches purified from different DBE mutant lines of Arabidopsis*

	Level of Crystallinity[a]	Amorphous-Crystalline Lamellae Repetition[b]
	%	nm
Ws	40	10.5
pu1-1	39	10.5
isa1-1	ND[c]	10.7
isa2-1	35	10.6
isa3-1	30	10.5
isa1-1 isa3-1	23	10.6
isa3-1 pu1-1	31	10.6

[a]As determined by WAXS. [b]As determined by SAXS. [c]Not determined.

of the starch content compared not only to the wild type but also to *isa3-1* and *pu1-1* mutants, whatever the length of the photoperiod and whatever the time of harvest in the day-night cycle. On the other hand, less severe modifications were recorded with respect to the other properties, such as a moderate increase in the number of very short chains of amylopectin and especially of DP3; no change of the amylopectin to amylose ratio; lower crystallinity of starch; but no modification of the signal intensity of the 9- to 10-nm repetition obtained by SAXS. The enhanced number of very short glucans (DP3-9) in the amylopectin of *isa3-1 pu1-1* (increase already visible for DP3-4 glucans in *isa3-1*) indicates a preference of the two DBEs for the hydrolytic cleavage of the very short glucans of amylopectin during starch degradation. The occurrence of these very short glucans in amylopectin may be a consequence of increased β-amylase activity as measured in both *isa3-1* and *isa3-1 pu1-1*. Because β-amylases are apparently essential for the degradation of transitory starch (Scheidig et al., 2002; Fulton et al., 2008) after phosphorylation of some Glc residues (Edner et al., 2007), it seems that ISA3 and PU1 are required for the elimination of the very short branched glucans that are actually not hydrolyzable by exo-amylases, whose activity is blocked by branches. The presence of a low yet significant amount of WSP that specifically increases at the end of the night in the *isa3-1 pu1-1* double mutant suggests that these soluble glucans likely result from another mechanism than that which leads to the massive accumulation of WSPs in *isa1-1*, *isa2-1*, or *isa2-1 pu1-1* (Delatte et al., 2005; Wattebled et al., 2005). We propose that these soluble glucans would come from an incomplete process of starch degradation in that specific mutant context (Delatte et al., 2006). The drop in crystallinity measured in both *isa3-1* and *isa3-1 pu1-1* could be related to an increase, day after day, of the phosphorylation level of the Glc residues subsequent to the lower starch degradation capacities in these lines. This hypothesis is in agreement with the results of Hejazi et al. (2008), which show that by their function of phosphorylation, glucan water dikinases most probably disorganize the crystalline structure of amylopectin to give access to the β-amylases. Another explanation would be that the increased number of DP3-4 glucans in amylopectin directly affects the organization of the crystalline lattice thus reducing the overall level of crystallites in starch.

Finally, the function of Iso1 (the DBE heteromultimeric protein complex formed by ISA1 and ISA2) in starch degradation is difficult to appreciate because of the epistatic behavior of synthesis toward degradation. However, as seen in Figure 2, the *isa3-1 pu1-1* double mutant is still able to degrade starch at night but at a lower rate than synthesis. The pattern of gene expression of both *ISA1* and *ISA2* genes does not correlate to that observed for enzymes of starch degradation (Smith et al., 2004; Li et al., 2007). Above all consideration regarding the catalytic properties of this enzyme, this might explain the low capacity of Iso1 to degrade starch. Moreover, the higher rate of starch degradation observed at night in *isa3-1* in comparison to *isa3-1 pu1-1* definitely shows the involvement of PU1 in starch degradation.

ISA1 and ISA3 Have Partially Redundant Functions toward Starch Synthesis

Leaf starch content at the end of the day was described as being strongly decreased in Arabidopsis *isa1-* mutants (Delatte et al., 2005; Wattebled et al., 2005). When grown with a photoperiod of 16 h under high light, the residual starch content was only 10% to 20% of the wild-type content (Table II). Combining both *isa1-1* and *isa3-1* mutations in one single individual further reduced starch accumulation to about 2% of the wild-type level (when plants are grown in the same conditions). It is thus a 5- to 10-fold reduction by comparison to *isa1-* or *isa2-* single mutants. The same behavior was observed when plants were cultivated with a 12-h photoperiod in climatic chambers, although the differences were less pronounced. The amount of WSPs that accumulate in *isa1-1 isa3-1* was roughly the same as in *isa1-1* and *isa2-1*, whatever the growth conditions used. This reduction of the starch content between *isa1-1* and *isa1-1 isa3-1* mutants establishes ISA3 as a net contributor of starch synthesis in which the effect is valued only when the major "synthetic DBE" (Iso1) is lacking. Also, this result definitely establishes the synthetic function of isoamylases as epistatic toward their function of starch degradation. If not, one would expect intermediary starch content in *isa1-1 isa3-1* compared to *isa1-1* and *isa3-1*. This is obviously not the case. The enhanced pullulanase activity observed in *isa1-1 isa3-1* may account for residual starch synthesis in this line. It is not clear yet whether this increase of pullulanase activity is a direct consequence of impaired isoamylase activity in the *isa1-1 isa3-1* mutant. Moreover, the mechanism by which pullulanase activity is increased is not known. However, such an increase was already observed by zymogram in the *isa2-1* mutant that is a strict phenocopy of the *isa1-1* mutant (indeed *isa1-*,

isa2-, and *isa1- isa2-* mutants display the same phenotype; Delatte et al., 2005; Wattebled et al., 2005). Such a behavior can be distinguished from that described in *sugary-1* mutants of maize and rice where pullulanase activity was reduced when the major isoamylase was impaired in the endosperm (Kubo et al., 1999; Dinges et al., 2003). This discrepancy may be a consequence of dissimilar regulation processes between transitory and storage starches or may highlight some differences in the nature of protein complexes in the two systems (isoamylases themselves are suspected to be organized in huge proteins complexes in vivo; Dauvillée et al., 1999; Utsumi and Nakamura, 2006).

Although it appears in the form of granules of a comparable size to that found in *isa1-1* (Fig. 9), the small amounts of insoluble polysaccharide that remain in the *isa1-1 isa3-1* double mutant are enriched in amylose, and the CLD profile of amylopectin shows a particular enrichment in very short glucans (DP3-8; Fig. 6E). In the same way, the CLD analysis of WSPs shows an even more dramatic enrichment in very short glucans especially for DP3-4 glucans. The increased accumulation of DP3-4 glucans in both WSPs and in the insoluble material of *isa1-1 isa3-1* is in good agreement with the abovementioned function of ISA3 that is related to the elimination of very short glucans during starch degradation. This result suggests that DBEs directly influence the structure of accumulating WSPs and that this influence equally applies to insoluble starch-like polysaccharides. Therefore, it can be argued that the intrinsic function of DBEs is not devoted to the clearing of WSP to avoid competition with starch synthesis but rather to adapt the structure of a primary soluble branched α-glucan (called preamylopectin by Ball et al. [1996]) to allow its further insolubilization and crystallization into mature amylopectin. If the function of DBEs was only dedicated to the degradation of WSPs accumulating during the soluble phase of amylopectin synthesis, one would not expect that they condition the structure of WSPs in circumstances where these soluble glucans are cyclically synthesized and degraded in 12-h-day/12-h-night conditions. In that case, WSPs would have been more or less the same in both *isa1-1* and *isa1-1 isa3-1* mutants (the structure of WSPs would then be conditioned by the combined action of starch synthases and branching enzymes). It is interesting to note here that pullulanase is by itself enough to degrade the WSPs that accumulate in *isa1-1 isa3-1* because WSP content reaches wild-type levels at the end of the night in 12-h photoperiod.

X-ray diffraction analysis reveals the considerable importance of these enzymes for the determination of crystallinity of starch. Indeed, our results show that the defect in *isa2-1* (note that *isa2-1* is a phenocopy of *isa1-1* regarding starch content and structure and leads to the same enzymatic defect of the Iso1 complex) compromises the possibility of synthesizing starch whose level of crystallinity is similar to that of the wild type (Table III). This effect is even more pronounced when the defect in Iso1 is combined to mutation in *ISA3*. Thus, the action of DBEs appears essential here to allow the correct crystalline organization of the amorphous and crystalline lamellae of amylopectin. When Iso1 is lacking (because of a mutation in either ISA1 or ISA2 or both), ISA3 seems able, at least partially, to fulfill its function. On the other hand, when Iso1 and ISA3 are simultaneously missing, the pullulanase does not seem proficient to allow the synthesis of starch crystallites. This hypothesis is strengthened by β-amylolysis experiments carried on amylopectin isolated from *isa1-1 isa3-1* and *isa3-1 pu1-1* mutants (Fig. 7). These analyses show that the core structure of amylopectin is modified in *isa1-1 isa3-1*, whereas it remains unchanged in *isa3-1 pu1-1*. Therefore, the distribution pattern of amylopectin branches is likely affected in *isa1-1 isa3-1*, which in turn affects crystallization.

For a Dual Function of Pullulanase in Leaf Starch Metabolism

To investigate the actual function of PU1 in the synthesis of the residual starch found in the *isa1-1 isa3-1* double mutant, the triple mutant *isa1-1 isa3-1 pu1-1* was constructed and analyzed. As expected from previous investigations, no remaining DBE activity was found in this triple mutant; Iso1, ISA3, and PU1 activity were all missing (Fig. 1, B and C). Because we know that ISA1 and ISA2 play identical functions in Arabidopsis and that mutation in either of these is sufficient to abolish the function of the isoamylase heteromultimeric enzyme, we infer that this triple mutant combination will result in a complete inhibition of all Arabidopsis DBE activities. Residual starch indeed falls down to less than 0.05% of the wild-type content and only 1/40th of the *isa1-1 isa3-1* content for plant cultivated in 16-h photoperiod. This result argues for a function of PU1 in starch synthesis although this function may seem marginal by comparison to Iso1 and ISA3 because of the low amounts of materials in consideration. Conversely, the WSP content in the triple mutant is high as already reported for both *isa1-1* and *isa1-1 isa3-1*. It must be underlined that even when *isa1-1 isa3-1 pu1-1* plants were left for up to 108 h in the dark, the WSPs content was still very high in comparison to *isa1-1* and *isa1-1 isa3-1* for which WSP content was back to almost zero after only 12 h in the dark. This result further argues for a complete wipeout of debranching activities in the triple mutant.

The CLD of both amylopectin and WSPs was affected in the triple mutant to a greater extent than in the *isa1-1 isa3-1* double mutant. The number of DP3-5 glucans increases considerably to represent up to 10% of the whole glucan content in amylopectin. The same modification was observed in WSPs, which shows a considerable increase in DP3-5 glucans compared to WSPs of *isa1-1*. Indeed, the phenotype observed in the *isa1-1 isa3-1* genotype is amplified in the *isa1-1 isa3-1 pu1-1* triple mutant combination, which is a further

argument for the implication of pullulanase in amylopectin synthesis although its level of implication remains very low in comparison to Iso1 and ISA3.

The question of the implication of DBEs in the priming of starch synthesis does not seem to be favorably confirmed by our results, at least in the sense generally accepted for the priming process. Indeed, our results show that DBEs condition the structure of both starch and WSPs, which accumulate in the corresponding mutants. It emerges here that syntheses of both macromolecules are interdependent. The gradual reduction of debranching activity is thus responsible for the progressive incapacity of the system to transform WSP into starch. In fact, WSPs do not seem to be side products of starch synthesis but indeed a mandatory route that allows the normal synthesis of amylopectin. In this context, DBEs obviously have an essential role for the formation of the starch granules by their actions on the formation of the amorphous and crystalline lamellae of amylopectin but they do not control the priming process of starch synthesis in a strict sense of the term. Indeed, the seeding of novel starch granules involves the production of three-dimensional scaffolds of unknown nature whereupon amylopectin aggregates to produce mature granules. Yet the seeds that are probably somewhat related to the hilum of starch granules are not expected to form a significant portion by weight of the final granule structure. A function affecting starch granule priming specifically is thus expected to potentially affect at best hilum structure and granule size and numbers. However, the structure of the amylopectin within these granules is in fact not expected to be modified or to be marginally affected through indirect effects originating from modifications of granule size distributions. However, we show here and in previous work that in all instances the structure of amylopectin in isoamylase-defective mutants defines some of the most profoundly affected structures documented. How can we thus explain the modification of starch granule sizes witnessed specifically in mutants defective for isoamylase? We believe this to be due to the abnormal production of glycogen particles in this case only (glycogen is not produced in *isa3-1* or *pu1-1* single or double mutants), which forms ideal 3-D scaffolds upon which some polysaccharides can aggregate to from starch-like granules (Putaux et al., 2006). This aggregation is assisted by the relatively inefficient trimming activities displayed by ISA3 and PU1 DBEs in the absence of isoamylase, as revealed by this work. In other systems where incompletely defective isoamylase mutants or antisense plants have been described or constructed, this effect is further amplified by the presence of the residual reduced or altered isoamylase. This is indeed expected to yield the presence of numerous small-size granules that may or may not be related to the normal process of starch granule seeding. An isoform of soluble starch synthase, the SS4, has recently been proposed to act as a major contributor of starch initiation in Arabidopsis leaves (Roldán et al., 2007). In this case starch granule numbers and sizes are dramatically affected in mutants with very little or no impact on amylopectin structure or WSP production.

MATERIALS AND METHODS

Chemicals

ADP-[U-^{14}C]Glc, [U-^{14}C]Glc-1-P, CL-2B Sepharose column, and Percoll were from Amersham Biosciences. ADP-Glc, Glc-1-P, and enzymes unless specified were from Sigma. The starch assay kit was purchased from Enzytec. The Suc, Fru, and Glc assay kit was from Megazyme.

Arabidopsis Lines, Growth Conditions, and Media

Wild-type Ws and Col-0 and mutant lines of Arabidopsis (*Arabidopsis thaliana*) were from the T-DNA mutant collections generated and/or maintained at INRA Versailles (Bechtold et al., 1993; Bouchez et al., 1993) and Nottingham Arabidopsis Stock Centre (NASC; Alonso et al., 2003). The *isa1-1* (line N542704) and *isa3-1* (line N604008) mutants were obtained from NASC. *pu1-1* (line CQU5) and *isa2-1* (line CTI15) were from INRA Versailles.

Plants were grown on peat-based compost and regularly watered to avoid drying. Seeds were previously incubated for at least 2 d in the dark at 4°C in 0.1% (w/v) Phytagar (Sigma) before sowing. Cultures were performed in a 16-h photoperiod (with a light intensity of 185 μmol m^{-2} s^{-1} in average) or a 12-h photoperiod (with a light intensity of 50 μmol m^{-2} s^{-1} in average) with temperature ranging from 16°C (during the night) to 21°C (during the illuminated period).

Iodine Staining of Leaves

Leaves harvested at the end of the light period were immediately immerged in ethanol 70% and heated to 80°C for 30 min with regular shaking to remove pigments. If required this operation was repeated until complete bleaching. Leaves were then impregnated with an iodine solution of KI 1% (w/v) I_2 0.1% (w/v), shortly rinsed in deionized water, and photographed.

RT-PCR Amplifications

Approximately 100 mg of fresh tissue was harvested during the light phase for total RNA extraction with the Plant RNeasy kit (Qiagen) following the supplier's instructions. Purified total RNA (20 ng) was used to perform RT-PCR amplifications using the OneStep RT-PCR kit (Qiagen) on the region spanning the T-DNA insertion site. Cycles of amplification were as follows: 3 min at 95°C; six cycles, 45″ at 95°C, 30″ at 63°C, and 1′30″ at 72°C with a recurrent reduction of 1°C of the annealing temperature at each cycle; 34 cycles, 45″ at 95°C, 30″ at 55°C, and 1′30″ at 72°C; and final extension 5 min at 72°C. The primers used for RT-PCR amplifications were the following: isa1 up en1, 5′-ACGGGGCTGATGAGAA; 5′-isa1 lo en 1, CTCTTCACCGAGATACTCGCAA; isa3 en up, 5′-AGGCCAATGGAGAAGGAGGAA; isa3 en lo, 5′-AAAGTAGTCGTGGGCGTTGAATG; pu1 en up, 5′-GGTCCCCTAGGTGCACATTTTACA; pu1 en lo, 5′-CCACGATTTTCAGGCTCAACAGTC; and 18S, Universal 18S (Ambion).

Extraction and Purification of Starch

Native starch was extracted from leaves harvested at the end of the light period (unless indicated) as described by Delvallé et al. (2005).

Extraction of Soluble Carbohydrates (WSPs, Glc, Fru, and Suc)

Leaves were harvested at the end of the light phase (unless indicated), immediately frozen in liquid nitrogen and stored at −80°C before extraction. WSPs and free sugars were extracted by the perchloric acid method as follows: leaves were broken down to rough pieces with a pestle directly in microtube, 500 μL of perchloric acid 0.7 M was added, and the samples were immediately homogenized with a polytron blender. The samples were then centrifuged for

15 min at 3,000*g* at 4°C. The soluble phase was collected and subsequently neutralized with KOH 2 M, MES 0.4 M, KCl 0.4 M. The potassium perchlorate precipitate was then removed by centrifugation at 16,000*g* for 15 min at 4°C. The supernatant was conserved at −80°C before use.

Determination of Starch and WSP Contents and Spectral Properties of the Iodine-Starch Complex

A full account of λ_{max} (maximal absorbance wavelength of the iodine polysaccharide complex) measure can be found in Delrue et al. (1992). Starch and WSP contents in leaves were determined after extraction (as described above) by the amyloglucosidase assay as described by Delvallé et al. (2005).

Determination of Glc, Suc, and Fru Contents

Glc, Suc and Fru contents were determined from leaf extract by the use of a specific kit (K-SUFRG; Megazyme) following the supplier's instructions.

Fractionation of Starch and WSP by Size Exclusion Chromatography

Amylopectin and amylose were separated from 1.5 to 2.0 mg native starch (unless indicated) by size exclusion chromatography on CL-2B column as fully described in Delvallé et al. (2005). The column was 60 cm in height and 0.5 cm in internal diameter. The elution of polysaccharide was performed at a flow rate of 12 mL/h. Collected fractions were of 300 μL in volume. Fractions were then analyzed by iodine staining (80 μL of sample combined to 20 μL of 2% [w/v] KI/0.2% [w/v] I_2 solution) for the detection of amylopectin and amylose.

Purified and lyophilized WSPs (2 mg) were dissolved in 2 mL of DMSO 10% (v/v) and loaded on a Sephadex TSK HW50 column (1 cm i.d. × 50 cm) equilibrated and eluted with DMSO 10% (v/v). Fractions of 2 mL were collected at a flow rate of 12 mL/h. Carbohydrates in the collected fractions were detected by phenol-sulfuric acid. Phenol (5%, 20 μL) was added to 20 μL of sample. After thorough shaking, 100 μL of concentrated sulfuric acid was added, and after gentle shaking the samples were incubated for 30 min at 80°C. Absorbance was determined at 490 nm.

CLD of Amylopectin and WSP

Amylopectin and WSP CLD were established by HPAEC-PAD (Dionex) after enzymatic debranching. Full description of the procedure can be found in Fontaine et al. (1993). HPAEC-PAD analysis was carried out on the Dionex DX6000 machine equipped with a CarboPac PA200 column (4 mm i.d. × 250 mm length).

β-Amylolysis of Purified Amylopectin

A full description of β-amylase degradation of amylopectin can be found in Delvallé et al. (2005).

Zymogram Techniques

Protein extracts were prepared from three to four leaves harvested at midday and kept on ice during the whole procedure of extraction. Leaves were homogenized in 100 μL of ice-cold buffer containing 100 mM MOPS, 1 mM EDTA, 1 mM dithiothreitol, glycerol 10% using a polytron blender (Tissue Tearor; Biospec Products). The homogenate was centrifuged twice for 10 min at 10,000*g* at 4°C. The supernatant was used for zymogram within the day.

Soluble starch synthase activities were as follows. Proteins (100 μg) from a leaf crude extract were loaded on a native PAGE (7.5% acrylamide) containing 0.3% of rabbit liver glycogen. After migration under native condition for 3 h at 4°C at 15 V cm^{-1}, the gel was incubated overnight at room temperature in the following buffer: 50 mM GlyGly/NaOH pH 9, 100 mM $(NH_4)_2SO_4$, 5 mM β-mercaptoethanol, 5 mM $MgCl_2$, 0.25 g L^{-1} BSA, and 1 mM ADP-Glc. Starch synthase activities were revealed by soaking the gel in iodine solution.

Starch modifying activities (hydrolases, branching enzymes, DBEs) were tested on glucan-containing gels as follows: 100 μg of leaf extract proteins was loaded onto a native PAGE (7.5% acrylamide) containing potato (*Solanum tuberosum*) soluble starch (Sigma) or maize (*Zea mays*) β-limit dextrin at 0.2% final concentration and separated for 3 h at 4°C and 15 V cm^{-1}. The gels were incubated overnight (for the gel with potato soluble starch) or 3 h (for the gel with maize β-limit dextrin) at room temperature in the following buffer: 50 mM sodium citrate, pH 6.0, 5 mM dithiothreitol, 50 mM Na_2HPO_4. The activities were revealed by soaking the gel into iodine solution (I_2 0.2% [w/v] and KI 2% [w/v]).

In Vitro Assays of Starch Metabolizing Enzymes

α- and β-Amylases, α-1,4 glucanotransferase (D-enzyme), glucan-phosphorylase, and AGPase activities were assayed as described by Delvallé et al. (2005).

SEM, TEM, and X-Ray Diffraction Measurements

A full account of electron microscopy techniques can be found in Delvallé et al. (2005). Diffraction diagrams were monitored by recording x-ray diffraction diagrams every 10 min on a Bruker D8 Discover diffractometer. Copper Kα1 radiation (λ = 1.5405 Å), produced in a sealed tube at 40 kV and 40 mA, was selected and parallelized using a Gobël mirror parallel optics system and collimated to produce a 500-mm beam diameter. WAXS analyses were performed on starch containing 20% H_2O (w.b.) after water sorption for 10 d in desiccators under partial vacuum. SAXS analyses were performed on starch containing 50% H_2O. Relative crystallinity was determined as described in Gerard et al. (2002).

Supplemental Data

The following materials are available in the online version of this article.

Supplemental Figure S1. Genotyping of mutant lines selected after crosses.

Supplemental Figure S2. Sephadex TSK HW50 profiles of soluble glucans extracted by the perchloric acid method from the *isa1-1 isa3-1 pu1-1* triple mutant cultivated in different lengths of photoperiod.

ACKNOWLEDGMENTS

We are grateful to Emilie Perrin for her excellent technical assistance in electron microscopy. We thank NASC and INRA of Versailles for providing us with the Arabidopsis mutants used in this work.

Received September 5, 2008; accepted September 22, 2008; published September 24, 2008.

LITERATURE CITED

Alonso JM, Stepanova AN, Leisse TJ, Kim CJ, Chen H, Shinn P, Stevenson DK, Zimmerman J, Barajas P, Cheuk R, et al (2003) Genome-wide insertional mutagenesis of *Arabidopsis thaliana*. Science **301:** 653–657

Ball S, Guan HP, James M, Myers A, Keeling P, Mouille G, Buléon A, Colonna P, Preiss J (1996) From glycogen to amylopectin: a model explaining the biogenesis of the plant starch granule. Cell **86:** 349–352

Bechtold N, Ellis J, Pelletier G (1993) In planta Agrobacterium mediated gene transfer by infiltration of adult Arabidopsis thaliana plants. C R Acad Sci Ser III Sci Vie **316:** 1194–1199

Bouchez D, Camilleri C, Caboche M (1993) A binary vector based on Basta resistance for in planta transformation of Arabidopsis thaliana. C R Acad Sci Ser III Sci Vie **316:** 1188–1193

Buléon A, Colonna P, Planchot V, Ball S (1998) Starch granules: structure and biosynthesis. Int J Biol Macromol **23:** 85–112

Dauvillée D, Colleoni C, Mouille G, Buléon A, Gallant DJ, Bouchet B, Morell MK, D'Hulst C, Myers AM, Ball SG (2001a) Two loci control phytoglycogen production in the monocellular green alga *Chlamydomonas reinhardtii*. Plant Physiol **125:** 1710–1722

Dauvillée D, Colleoni C, Mouille G, Morell MK, D'Hulst C, Wattebled F, Liénard L, Delvallé D, Ral J-P, Myers AM, et al (2001b) Biochemical characterization of wild-type and mutant isoamylases of *Chlamydomonas*

reinhardtii supports a function of a multimeric enzyme organization in amylopectin maturation. Plant Physiol **125:** 1723–1731

Dauvillée D, Colleoni C, Shaw E, Mouille G, D'Hulst C, Morell M, Samuel MS, Bouchet B, Gallant DJ, Sinskey A, Ball S (1999) Novel, starch-like polysaccharides are synthesized by an unbound form of granule-bound starch synthase in glycogen-accumulating mutants of *Chlamydomonas reinhardtii*. Plant Physiol **119:** 321–330

Delatte T, Trevisan M, Parker ML, Zeeman SC (2005) Arabidopsis mutants Atisa1 and Atisa2 have identical phenotypes and lack the same multimeric isoamylase, which influences the branch point distribution of amylopectin during starch synthesis. Plant J **41:** 815–830

Delatte T, Umhang M, Trevisan M, Eicke S, Thorneycroft D, Smith SM, Zeeman SC (2006) Evidence for distinct mechanisms of starch granule breakdown in plants. J Biol Chem **281:** 12050–12059

Delrue B, Fontaine T, Routier F, Decq A, Wieruszeski J-M, van den Koornhuyse N, Maddelein M-L, Fournet B, Ball S (1992) Waxy Chlamydomonas reinhardtii: monocellular algal mutants defective in amylose biosynthesis and granule-bound starch synthase activity accumulate a structurally modified amylopectin. J Bacteriol **174:** 3612–3620

Delvallé D, Dumez S, Wattebled F, Roldan I, Planchot V, Berbezy P, Colonna P, Vyas D, Chatterjee M, Ball S, et al (2005) Soluble starch synthase I: a major determinant for the synthesis of amylopectin in Arabidopsis thaliana leaves. Plant J **43:** 398–412

Dinges JR, Colleoni C, James MG, Myers AM (2003) Mutational analysis of the pullulanase-type debranching enzyme of maize indicates multiple functions in starch metabolism. Plant Cell **15:** 666–680

Edner C, Li J, Albrecht T, Mahlow S, Hejazi M, Hussain H, Kaplan F, Guy C, Smith SM, Steup M, et al (2007) Glucan,water dikinase activity stimulates breakdown of starch granules by plastidial beta-amylases. Plant Physiol **145:** 17–28

Fontaine T, D'Hulst C, Maddelein ML, Routier F, Marianne-Pepin T, Decq A, Wieruszeski JM, Delrue B, van den Koornhuyse N, Bossu JP, et al. (1993) Toward an understanding of the biogenesis of the starch granule. Evidence that Chlamydomonas soluble starch starch synthase II controls the synthesis of intermediate size glucans of amylopectin. J Biol Chem **268:** 16223–16230

Fulton DC, Stettler M, Mettler T, Vaughan CK, Li J, Francisco P, Gil M, Reinhold H, Eicke S, Messerli G, et al. (2008) Beta-AMYLASE4, a noncatalytic protein required for starch breakdown, acts upstream of three active beta-amylases in *Arabidopsis* chloroplasts. Plant Cell **20:** 1040–1058

Gerard C, Colonna P, Buléon A, Planchot V (2002) Order in maize mutant starches revealed by mild acid hydrolysis. Carbohydr Polym **48:** 131–141

Hejazi M, Fettke J, Haebel S, Edner C, Paris O, Frohberg C, Steup M, Ritte G (2008) Glucan, water dikinase phosphorylates crystalline maltodextrins and thereby initiates solubilization. Plant J **55:** 323–334

Hennen-Bierwagen TA, Liu F, Marsh RS, Kim S, Gan Q, Tetlow IJ, Emes MJ, James MG, Myers AM (2008) Starch biosynthetic enzymes from developing maize endosperm associate in multisubunit complexes. Plant Physiol **146:** 1892–1908

Hovenkamp-Hermelink J, Jacobsen E, Ponstein A, Visser R, Vos-Scheperkeuter G, Bijmolt E, de Vries J, Witholt B, Feenstra W (1987) Isolation of an amylose-free starch mutant of the potato (*Solanum tuberosum* L.). Theor Appl Genet **75:** 217–221

Hussain H, Mant A, Seale R, Zeeman S, Hinchliffe E, Edwards A, Hylton C, Bornemann S, Smith AM, Martin C, et al (2003) Three isoforms of isoamylase contribute different catalytic properties for the debranching of potato glucans. Plant Cell **15:** 133–149

James MG, Robertson DS, Myers AM (1995) Characterization of the maize gene *sugary1*, a determinant of starch composition in kernels. Plant Cell **7:** 417–429

Jenkins PJ, Cameron RE, Donald AM (1993) A universal feature in the starch granules from different botanical sources. Starch-Stärke **45:** 417–420

Kubo A, Fujita N, Harada K, Matsuda T, Satoh H, Nakamura Y (1999) The starch-debranching enzymes isoamylase and pullulanase are both involved in amylopectin biosynthesis in rice endosperm. Plant Physiol **121:** 399–410

Kubo A, Rahman S, Utsumi Y, Li Z, Mukai Y, Yamamoto M, Ugaki M, Harada K, Satoh H, Konik-Rose C, et al (2005) Complementation of *sugary-1* phenotype in rice endosperm with the wheat isoamylase1 gene supports a direct role for isoamylase1 in amylopectin biosynthesis. Plant Physiol **137:** 43–56

Li L, Ilarslan H, James MG, Myers AM, Wurtele EV (2007) Genome wide co-expression among the starch debranching enzyme genes *AtISA1*, *AtISA2*, and *AtISA3* in Arabidopsis thaliana. J Exp Bot **58:** 3323–3342

Morell MK, Li Z, Regina A, Rahman S, D'Hulst C, Ball SG (2006) Control of starch biosynthesis in vascular plants and algae. *In* WC Plaxton, MT McManus, eds, Control of Primary Metabolism in Plants. Annual Plant Reviews, Vol 22. Blackwell Publishing, Oxford, pp 258–289

Mouille G, Maddelein ML, Libessart N, Talaga P, Decq A, Delrue B, Ball S (1996) Preamylopectin processing: a mandatory step for starch biosynthesis in plants. Plant Cell **8:** 1353–1366

Myers AM, Morell MK, James MG, Ball SG (2000) Recent progress toward understanding biosynthesis of the amylopectin crystal. Plant Physiol **122:** 989–997

Nakamura T, Yamamori M, Hirano H, Hidaka S, Nagamine T (1995) Production of waxy (amylose-free) wheats. Mol Gen Genet **248:** 253–259

Putaux JL, Potocki-Véronèse G, Remaud-Simeon M, Buleon A (2006) α-D-glucan-based dendritic nanoparticles prepared by in vitro enzymatic chain extension of glycogen. Biomacromolecules **7:** 1720–1728

Roldán I, Wattebled F, Lucas M, Delvallé D, Planchot V, Ricardo Pérez SJ, Ball SG, D'Hulst C, Mérida A (2007) The phenotype of soluble starch synthase IV defective mutants of *Arabidopsis thaliana* suggests a novel function of elongation enzymes in the control of starch granule formation. Plant J **49:** 492–504

Scheidig A, Fröhlich A, Schulze S, Lloyd JR, Kossmann J (2002) Down-regulation of a chloroplast-targeted β-amylase leads to a starch-excess phenotype in leaves. Plant J **30:** 581–591

Smith SM, Fulton DC, Thorneycroft D, Chapple A, Dunstan H, Hylton C, Zeeman SC, Smith AM (2004) Diurnal changes in the transcriptome encoding enzymes of starch metabolism provide evidence for both transcriptional and posttranscriptional regulation of starch metabolism in Arabidopsis leaves. Plant Physiol **136:** 2687–2699

Tetlow IJ, Beisel KG, Cameron S, Makhmoudova A, Liu F, Bresolin NS, Wait R, Morell MK, Emes MJ (2008) Analysis of protein complexes in wheat amyloplasts reveals functional interactions among starch biosynthetic enzymes. Plant Physiol **146:** 1878–1891

Utsumi Y, Nakamura Y (2006) Structural and enzymatic characterization of the isoamylase1 homo-oligomer and the isoamylase1-isoamylase2 hetero-oligomer from rice endosperm. Planta **225:** 75–87

Wattebled F, Dong Y, Dumez S, Delvallé D, Planchot V, Berbezy P, Vyas D, Colonna P, Chatterjee M, Ball S, et al (2005) Mutants of Arabidopsis lacking a chloroplastic isoamylase accumulate phytoglycogen and an abnormal form of amylopectin. Plant Physiol **138:** 184–195